Phase Coexistence during Surface Phase Transitions

J. B. Hannon, F.-J. Meyer zu Heringdorf, J. Tersoff, and R. M. Tromp
IBM Research Division, T.J. Watson Research Center, P.O. Box 218, Yorktown Heights, New York 10598
(Received 19 December 2000)

In contrast to standard thermodynamic models, we observe phase coexistence over an extended temperature range at a first-order surface phase transition. We have measured the domain evolution of the Si(111)-(7 × 7) to (1 × 1) phase transition with temperature, using low-energy electron microscopy. Comparison with detailed, quantitative theoretical predictions shows that coexistence is due to long-range elastic and electrostatic domain interactions. Phase coexistence is predicted to be a universal feature of surface phase transitions.

DOI: 10.1103/PhysRevLett.86.4871 PACS numbers: 68.35.Md, 05.70.Np, 68.35.Rh, 68.37.Nq

One of the most important and fundamental results in thermodynamics is the Gibbs phase rule. For a single element at constant temperature and pressure, this rule states that there can be no coexistence of different phases. In equilibrium, as the temperature is varied the entire system changes discontinuously from one phase to the other. However, this rule does not include the possibility of long-range interactions. Twenty years ago, Marchenko suggested that there could be no true first-order phase transition at a solid surface [1]. Any two surface phases must have different surface stress, and the resulting elastic interactions have such long range that they preclude a sharp transition even in the thermodynamic limit. A similar electrostatic interaction arises from the work function difference of the two phases [2].

Here we present the first quantitative evidence to support this prediction. We examine the well-known phase transition of the Si(111) surface from an ordered (7 × 7) structure to a disordered ("1 × 1") phase at a temperature $T_c \approx 1135$ K. A key feature of this transition is that phase coexistence is observed over a broad temperature range near T_c, a fact that led to debate as to the order of the transition [3,4] and speculation about the origin of the coexistence [5]. Here we measure the actual domain structure and compare it to the predictions of theory. The results show conclusively that long-range elastic and electrostatic interactions are responsible for the phase coexistence. In addition, we derive a simple expression for the entropy difference between the phases in terms of measured electronic and elastic properties of the surface.

Of course, when volume rather than pressure is held constant in bulk systems, phase coexistence can occur. There has been confusion about how this applies to surfaces [5]. For a surface phase transition, the lattice constants of the two phases are each independently fixed by the bulk. Therefore, there is no surface analog of constant-volume phase coexistence.

Images of the Si(111) surface were obtained by low-energy electron microscopy (LEEM) [6], using 10 eV electrons reflected specularly from the surface. The microscope used here incorporates a novel 90° magnetic separator, and is capable of a lateral resolution better than 5 nm [7]. The sample temperature was calibrated to the heating power using an optical pyrometer.

The surface is very slightly misoriented relative to the (111) atomic planes, giving a staircase of (111) terraces and atomic steps. Every step on the surface is a phase boundary, consistent with the fact that the (7 × 7) structure nucleates at the upper edge of steps [4]. Phase boundaries not attached to a step tend to facet along $\langle 1\bar{1}0\rangle$, their low-energy direction. Thus, we can obtain a simple stripe geometry by choosing a surface misoriented towards the $\langle \bar{1}\bar{1}2\rangle$ direction, so that steps are parallel to the low-energy phase boundary orientation. Then, as the sample is cooled slowly from above T_c, a one-dimensional array of parallel phase boundaries forms (Fig. 1). Each domain is bounded

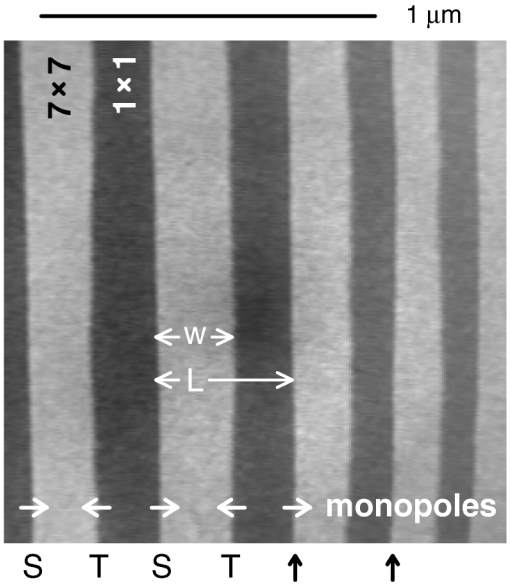

FIG. 1. Bright-field LEEM image of the Si(111) surface at the phase transition temperature. The local miscut is towards the $\langle \bar{1}\bar{1}2\rangle$ direction so that the steps (which all step up to the right) are parallel to the low-energy domain boundaries. The (7 × 7) areas appear brighter than the (1 × 1) areas due to the reflectivity difference for 10 eV electrons. Phase boundaries are found alternately at step edges (S) and on the terraces (T). Dark arrows indicate the terrace analyzed in Fig. 2. White arrows show the orientation of phase boundary force monopoles.

by two types of phase boundaries. One phase boundary is pinned to the $\langle \bar{1}\bar{1}2 \rangle$ step edge (marked "S" in Fig. 1). The other phase boundary is in the middle of the terrace ("T") and does not involve a surface step.

A sequence of images recorded at sample temperatures near T_c is shown in Fig. 2(a). By imaging both when cooling from above T_c and heating from below T_c, we verify that the surface structure has equilibrated. As the temperature is raised, the (7 × 7) domains shrink towards the upper sides of the step edges. The location of the terrace phase boundaries relative to the steps can be expressed in terms of the asymmetry parameter $p = (\frac{2w}{L} - 1)$, where w is the width of the (7 × 7) domain, and L is the terrace width (Fig. 1). Complete coverage of the terrace by (7 × 7) corresponds to $p = +1$, while $p = -1$ for pure (1 × 1). For comparison with theory, it is convenient to plot the quantity $\tan(p\pi/2)$ versus temperature, rather than p directly. Also, we plot temperature relative to the temperature T_0 ($\approx T_c$) at which the domains have equal widths ($p = 0$).

Figure 2(b) shows that near T_c, $\tan(p\pi/2)$ is approximately proportional to $T - T_0$, with a slope of $-0.12\ \mathrm{K}^{-1}$. At higher temperatures, where the width of the (7 × 7) domain is less than about 100 nm [point D in Fig. 2(b)], p decreases rapidly with T.

The area fractions of the two domains also depend strongly on the terrace width L. The dependence of $\tan(p\pi/2)$ on L is shown in Fig. 3 for four temperatures above T_c. The measurements are made on a region of the surface where the terrace width changes continuously, but where the steps and phase boundaries are still parallel. Despite some scatter in the data, for each temperature $\tan(p\pi/2)$ is proportional to L over a broad range of terrace widths.

Any model of the phase coexistence must reproduce the linear dependence of $\tan(p\pi/2)$ on terrace width and temperature near $p = 0$. In addition, the dependence on terrace size rules out any explanation not involving long-range interactions.

The nature of the long-range interactions between phase boundaries (and other line defects such as steps) is well understood [1,2,8–11]. When two phases have different surface stress, the boundary corresponds to a line of force (a "force monopole") $\mathbf{F} = \nabla \cdot \sigma$, where σ is the (two-dimensional) surface stress tensor. In addition, any

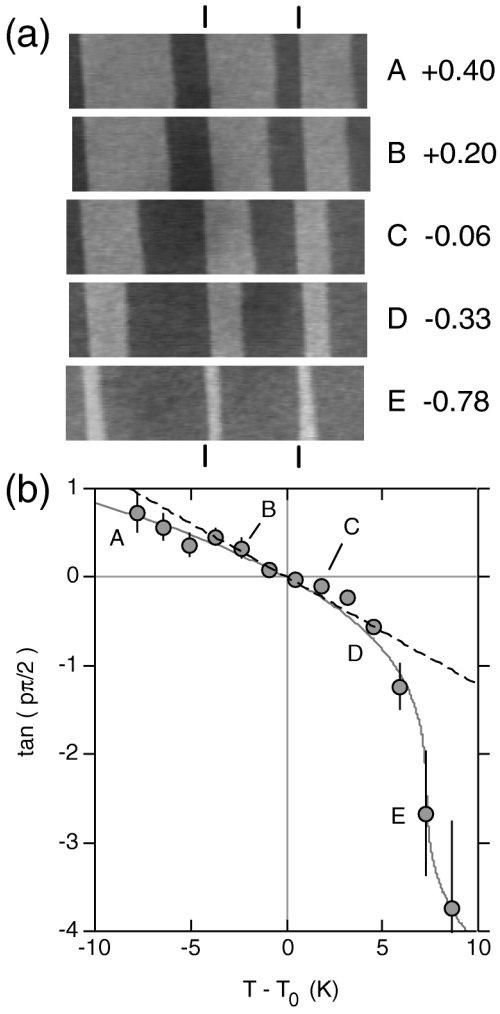

FIG. 2. (a) LEEM images of the 310-nm-wide terrace indicated in Fig. 1 for selected temperatures near T_c. Each image is labeled by the corresponding value of the asymmetry parameter p. The horizontal dimension of the images is 1.0 μm. (b) Temperature dependence of $\tan(p\pi/2)$ near T_c for the terrace shown in (a). The slope of the dashed line is $-0.12\ \mathrm{K}^{-1}$. The solid curve is a fit to the model described by Eq. (1).

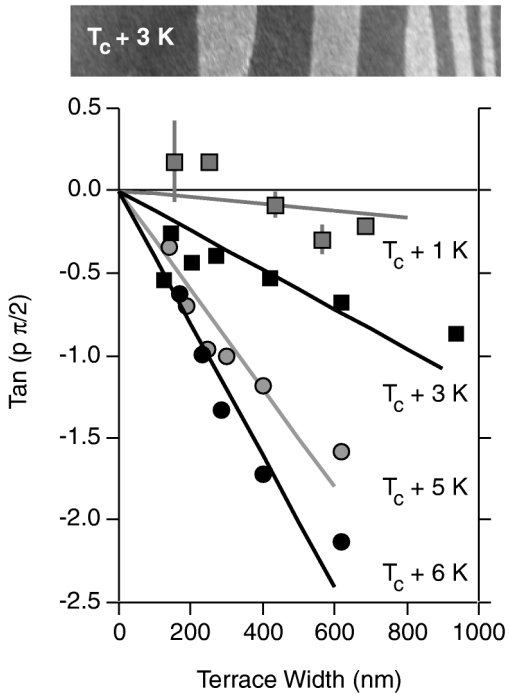

FIG. 3. Variation of $\tan(p\pi/2)$ with terrace width computed from images at four different temperatures above T_c. The inset is a 3.0 × 0.5 μm image of the surface at $T = T_c + 3$ K, illustrating the variation in terrace widths.

localized defect such as a step will have a "force dipole," as well as higher-order multipole moments [11]. The interaction between such forces at a surface is a standard result in elasticity [12]. The orientation of the measured [13] elastic force monopoles for Si(111) is shown in Fig. 1.

For metals, the electrostatic interactions between phase boundaries and other defects have the same form, with the simplification that the tensor surface stress is replaced by the scalar work function. We approximate the electrostatic interactions for Si(111) using formulas derived for metals, since the dielectric constant is large, and the silicon bulk free carrier density near T_c is large.

Then the energy E per unit area depends on p as

$$E = \frac{C_0}{L} + \frac{\Delta S(T - T_c)p}{2} - \frac{2C_m}{L}\ln\left[\frac{L}{\pi a}\cos\left(\frac{p\pi}{2}\right)\right] + \frac{C_d}{L^2}\tan\left(\frac{p\pi}{2}\right) - \frac{8C_r}{L^3}\left[\frac{1}{(1+p)^2} + \frac{1}{(1-p)^2}\right]. \quad (1)$$

The constant C_0 includes the creation energies of the steps and phase boundaries. The difference in surface free energy between the two phases is $\Delta S(T - T_c)$, where we treat the entropy difference ΔS between the phases as constant over our temperature range.

Long-range interactions enter through the last three terms. The term with C_m represents the interaction between elastic and/or electrostatic monopoles at the phase boundaries. (The atomic-scale cutoff parameter a is required for a consistent formulation, but has no effect on p.) The term with C_d represents the next-longest range interaction in the multipole expansion, that between the monopoles and the force dipoles at both step and terrace phase boundaries. The C_r term approximates a short-range repulsion between the phase boundaries.

In equilibrium, the surface adopts the value of p that minimizes the energy E in Eq. (1); thus we can obtain an explicit relationship between p and T by solving $dE/dp = 0$. A comparison between the full theory and experiment is shown in Fig. 2(b), with $C_m = 0.31$ meV/Å, $C_d = 0.81$ eV, and $C_r = 8.6$ eV Å.

On wide terraces near T_c, the contribution from the C_d and C_r terms to $E(p)$ is small, and $\tan(p\pi/2)$ is expected to vary linearly with temperature and terrace width:

$$\tan(p\pi/2) \approx -\frac{L\Delta S}{2\pi C_m}(T - T_c). \quad (2)$$

Thus in Fig. 2(b), the slope of the curve near $T = T_0$ (dashed line) gives a direct measure of the entropy difference between the two surface phases, relative to C_m. Within a few degrees of T_0 the dependence of $\tan(p\pi/2)$ on T is linear, with a slope of -0.12 K^{-1}. In combination with an independent determination of C_m, described below, this provides a measure of the entropy difference ΔS, which is a very fundamental but elusive parameter.

C_m includes elastic and electrostatic contributions, $C_m = C_\lambda + C_\phi$. The elastic contribution is $C_\lambda = (\lambda_m)^2(1 - \nu^2)/\pi Y$, where λ_m is the difference in surface stress between the two phases, ν is Poisson's ratio, and Y is Young's modulus. The electrostatic interaction may be similarly described as arising from the difference in the "surface dipole" between the two phases, $C_\phi = (\Delta\phi)^2/8\pi^2$ (in electrostatic units) [2], where $\Delta\phi$ is the difference in work function between the two surface phases. Using transmission electron microscopy, Twesten and Gibson measured $\lambda_m = 30 \pm 5$ meV/Å^2, or $C_\lambda = 0.28$ meV/Å [13]. The work function difference at T_c can be estimated using LEEM by observing the transition to total reflection as the beam energy is lowered. With this technique we find $\Delta\phi = 0.15 \pm 0.03$ eV, or $C_\phi = 0.02$ meV/Å, suggesting that elastic relaxation dominates the interaction between phases. With these values, the measured slope at $p = 0$ corresponds to an entropy difference between the (1×1) and (7×7) structures of only $0.011k_B/(1 \times 1)$ cell, or a latent heat of 1.1 meV/(1×1) cell. We must emphasize that the entropy difference is proportional to λ_m^2, and is therefore sensitive to systematic errors in the measured stress [14].

The small value of ΔS is perhaps surprising, since one phase has long-range order and the other does not. A simple model by Bartelt [15] suggests an entropy of order $0.25k_B$ per cell for the (1×1) phase. This entropy represents the disorder in a $\sqrt{3} \times \sqrt{3}$ adatom structure with about one out of three adatoms missing. The (7×7) phase includes an adatom structure, and its vacancy formation energy is expected to be very similar to that of the $\sqrt{3}$ structure [16]; therefore, the adatom vacancy concentration and the entropy should be comparable in the two phases. Thus the entropy difference between the phases is expected to be much smaller than the absolute entropy of either phase.

The value of C_d determined from the fit shown in Fig. 2(b) can be used to estimate the magnitude of the force dipoles at the phase boundaries. Specifically, $C_d = C_\lambda \pi \lambda_d/\lambda_m$, where λ_d is the sum of the dipoles at the step and terrace boundary. The fit corresponds to $\lambda_d \sim 25$ eV/Å [17]. Despite the seemingly large value of λ_d, the contribution to the surface energy from long-range forces [Eq. (1)] is small. Over the range $T_c - 5$ to $T_c + 5$ K, the combined change in surface energy arising from *all* elastic effects amounts to less than 1 μeV per (1×1) cell.

Throughout our analysis we have assumed that there is one pair of phase boundaries per surface step. This is true for Si(111) over the range of temperature and step spacing in our experiment. However, it is important to consider also what would happen in the absence of steps. For instance, on very large terraces, (7×7) domains form a random granular network in which phase boundaries are not associated with steps. When heated from below T_c, the (1×1) regions appear and broaden between the (7×7) domains, which could be described as domain wall

premelting. Very similar observations were made by Feenstra *et al.* in a study of the Ge(111)-$c(2 \times 8)$ to (1×1) phase transition [18].

For a step-free surface, and neglecting any possible force dipoles at the phase boundaries, the equilibrium structure is determined by simultaneously minimizing Eq. (1) with respect to L and p. Again, the result is phase coexistence over a finite temperature range centered on T_c. Within this range, the equilibrium spacing of domains (the periodicity) is

$$L = \left[\left(\frac{1}{L_{\min}} \right)^2 - \left(\frac{\Delta S(T - T_c)}{2\pi C_m} \right)^2 \right]^{-1/2}, \qquad (3)$$

where the minimum period $L_{\min} = ae\pi \exp(C_b/C_m)$ occurs at T_c, and C_b is the terrace domain boundary creation energy.

This provides a natural explanation for phase coexistence on large, step-free terraces, and for its manifestation as domain boundary premelting. As the system is cooled below T_c, the ordered domain size grows until the system eventually falls out of equilibrium; and below the coexistence range the disordered regions disappear, leaving only domain boundaries. Upon heating, the disordered phase first appears at these domain boundaries. However, this is fundamentally different from classical boundary premelting, because in equilibrium the disordered phase would appear even without preexisting domain boundaries. While Eq. (3) was derived for a one-dimensional array of domains, similar behavior is expected for two-dimensional arrays [19].

In conclusion, we have shown that long-range interactions lead to surface phase coexistence over a range of temperature. Measurements of domain evolution for Si(111) are in quantitative agreement with theory, and provide a measure of the latent heat of the transition. The same effects explain previous observations of surface phase coexistence in other systems, confirming the universal nature of the phenomenon.

We are grateful to Norm Bartelt for providing the results of his entropy calculation and for valuable discussions during the course of this work. Frank Meyer zu Heringdorf acknowledges support from the Alexander von Humboldt Foundation under the Feodor-Lynen program.

[1] V. I. Marchenko, JETP Lett. **33**, 382 (1981).
[2] D. Vanderbilt, Surf. Sci. Lett. **268**, L300 (1992).
[3] N. Osakabe, K. Yagi, and G. Honjo, Jpn. J. Appl. Phys. **19**, L309 (1980); P. A. Bennet and M. B. Webb, Surf. Sci. **104**, 74 (1981); Y. Tanishiro, K. Takayanagi, and K. Yagi, Ultramicroscopy **11**, 95 (1983).
[4] W. Telieps and E. Bauer, Surf. Sci. **162**, 163 (1985).
[5] J. Chevrier, Le Thanh Vinh, and A. Cruz, Surf. Sci. Lett. **268**, L261 (1992).
[6] E. Bauer, Rep. Prog. Phys. **57**, 895 (1994).
[7] R. M. Tromp, M. Mankos, M. C. Reuter, A. W. Ellis, and M. Copel, Surf. Rev. Lett. **5**, 1189 (1998).
[8] O. L. Alerhand, D. Vanderbilt, R. D. Meade, and J. D. Joannopoulos, Phys. Rev. Lett. **61**, 1973 (1988).
[9] E. Pehlke and J. Tersoff, Phys. Rev. Lett. **67**, 465 (1991).
[10] V. I. Marchenko and A. Ya. Parshin, Sov. Phys. JETP **52**, 129 (1981).
[11] D. J. Srolovitz, J. P. Hirth, Surf. Sci. **255**, 111 (1991).
[12] L. D. Landau and E. M. Lifshitz, *Theory of Elasticity* (Butterworth-Heinemann, Oxford, 1997).
[13] R. D. Twesten and J. M. Gibson, Phys. Rev. B **50**, 17 628 (1994).
[14] Analysis of phase boundary wandering [J. B. Hannon and R. M. Tromp (to be published)] suggests that the surface stress difference could be as large as 60 meV/Å^2, corresponding to an entropy difference of $0.05k_B$ per (1×1) cell.
[15] N. C. Bartelt (unpublished).
[16] J. E. Northrup, in *Proceedings of the 18th International Conference on the Physics of Semiconductors, Stockholm, 1986,* edited by O. Engstrom (World Scientific, Singapore, 1987), p. 61.
[17] The uncertainties in C_d and C_r are large for two reasons. First, the uncertainty in the data at high temperature is large because the (7×7) stripe is very narrow. Second, the values of C_d and C_r are correlated because the attractive dipole-monopole interaction (at high T) counteracts the short-ranged repulsion.
[18] R. M. Feenstra, A. J. Slavin, G. A. Held, and M. A. Lutz, Phys. Rev. Lett. **66**, 3257 (1991).
[19] K. O. Ng and D. Vanderbilt, Phys. Rev. B **52**, 2177 (1995).